Dynamic full-field optical coherence tomography as complementary tool in fungal diagnostics

Thomas Maldiney, Jean-Marie Chassot, Claude Boccara, Mathieu Blot, Lionel Piroth, Pierre-Emmanuel Charles, Dea Garcia-Hermoso, Fanny Lanternier, Frédéric Dalle, Marc Sautour

Version of Record: https://www.sciencedirect.com/science/article/pii/S1156523322000609
Manuscript_68d45703ceb248da91b921e71acf9160

Dynamic Full-Field Optical Coherence Tomography as Complementary Tool in Fungal Diagnostics

Thomas Maldiney[1,2*], Jean-Marie Chassot[3], Claude Boccara[3], Mathieu Blot[2,4], Lionel Piroth[4,5], Pierre-Emmanuel Charles[2,6], Dea Garcia-Hermoso[7], Fanny Lanternier[7,8], Frédéric Dalle[9,10], Marc Sautour[9,10]

[1]Department of Intensive Care Medicine, William Morey General Hospital, Chalon-sur-Saône, France

[2]Lipness team, INSERM Research Center LNC-UMR1231, University of Burgundy, Dijon, France

[3]Institut Langevin, ESPCI Paris, PSL University, CNRS, 75005 Paris, France

[4]Infectious Diseases Department, Dijon Bourgogne University Hospital, Dijon, France

[5]INSERM, CIC1432, Clinical Epidemiology unit, Dijon, France

[6]Department of Intensive Care, Dijon Bourgogne University Hospital, Dijon, France

[7]Institut Pasteur, Université de Paris, Molecular Mycology Unit, National Reference Center for Invasive Mycoses and Antifungals (NRCMA), UMR 2000, CNRS, Paris, France

[8]Department of Infectious Diseases and Tropical Medicine, Necker-Enfants Malades Hospital, Assistance Publique-Hôpitaux de Paris, Paris, France

[9]Department of Parasitology/Mycology, Dijon Bourgogne University Hospital, 21000 Dijon, France

[10]UMR PAM A 02.102 Procédés Alimentaires et Microbiologiques, Univ. Bourgogne Franche-Comté, AgroSup Dijon, Dijon, France

*** Correspondence :**
thomas.maldiney@ch-chalon71.fr

Keywords: Full-Field Optical Coherence Tomography, Fungal Diagnostics, Invasive Fungal Infections, Dynamic Contrast, Fungal Metabolism.

Abstract

Histopathology and microscopic examination of infected tissue are the gold standards to prove the diagnosis of invasive fungal infection (IFI). Yet, they suffer from essential limitations that hamper rapid diagnosis and require the future development of new imaging tools dedicated to fungal diagnostics. To this end, the present work introduces the first use of dynamic full-field optical coherence tomography (D-FF-OCT) for the visualization of microscopic filamentous fungi. Data collected from the observation of three different fungal species (*Nannizzia gypsea*, *Aspergillus fumigatus* and *Rhizopus arrhizus*) confirm the ability of D-FF-OCT to visualize not only the main structures of all selected fungal species (hyphae, spores, conidia, sporulating structures), but also the metabolic activity of the organisms, which could provide additional help in the future to better characterize the signature of each fungal structure. These results demonstrate how D-FF-OCT could serve as potential complementary tool for rapid diagnosis of IFI in both intensive and non-intensive care units.

1 Introduction

Invasive fungal infections (IFI) are associated with a large morbi-mortality in both immunocompromised and critically ill patients [1,2]. According to a recent update from the European Organization for Research and Treatment of Cancer and the Mycoses Study Group Education and Research Consortium (EORTC/MSGERC), IFI diagnosis mostly relies on the combination of host factors, clinical features, as well as mycological evidence [3]. Indeed, despite tremendous progress regarding the validation and implementation of polymerase chain reaction (PCR)-based methods as essential criteria for probable invasive fungal disease, histopathology or microscopic examination of infected tissue remain gold standards for the diagnosis of proven IFI [4,5]. Yet, the absolute necessity to obtain a timely and proven diagnosis in specific cases of IFI requires to address many challenges and pitfalls in histopathology or other culture-independent solutions dedicated to the diagnosis of fungal diseases [6]. As an example, a convenient tool to allow a rapid and easy differential diagnosis between invasive aspergillosis and mucormycosis *in situ* would help both infectious disease specialists and surgeons to choose the best therapeutic option between exclusive medical treatment and the adjunction of urgent extensive surgery. One of the solutions would be to uncover a technology able to assess the invasive nature of a fungal species within one superficial or deep tissue sample in a few minutes only, and without any coloration step.

As full-field optical coherence tomography (FF-OCT), dynamic full-field optical coherence tomography (D-FF-OCT) relies on broad band interference microscopy and provides ultra-high resolution structure images of biological tissues [7] as well as subcellular metabolic contrast within a few minutes [8]. In comparison to standard OCT or confocal microscopy, D-FF-OCT was shown to improve spatial resolution up to ten times [9]. Apart from recent medical applications [7,10,11], most studies have considered the potential importance of D-FF-OCT as imaging alternative for extemporaneous analysis in oncologic interventions and future way to easier and quicker surgical pathology [12]. However and excluding previous attempts to visualize *Malassezia* Folliculitis [13], cutaneous larva migrans [14] and even *Sarcoptes scabiei* infestation [15] with OCT systems displaying neither high spatial resolution nor the ability to follow dynamic contrast, there has been to our knowledge no reported attempt to exploit high-definition D-FF-OCT in fungal diagnostics. The present work introduces the first application of D-FF-OCT for the observation of different filamentous fungal species *in vitro*. We address the hypothesis that D-FF-OCT could help both physicians and pathologists to circumvent common pitfalls and develop timely and automated histopathology analysis dedicated to the diagnosis of IFI.

2 Materials and Methods

2.1 Fungal strains

Nannizzia gypsea (NG), *Aspergillus fumigatus* (AF) and *Rhizopus arrhizus* (RA) were isolated from patients and identified by mass spectrometry (MALDI-TOF) in the laboratory of Parasitology-Mycology of Dijon Bourgogne University Hospital. The strains were cultivated on Sabouraud dextrose agar (BioMérieux SA, Marcy-l'Etoile, France) and incubated at 28°C for proper growth.

2.2 FF-OCT standard and dynamic contrast imaging

As described elsewhere [10] and presented in Figure 1, D-FF-OCT images were acquired with a commercially available D-FF-OCT apparatus (Light-CTScanner, LLTech - Aquyre

Bisciences, Paris, France) [16]. Briefly, a conventional halogen source with short temporal coherence length was used for illumination to ensure an axial resolution of 1 µm (Figure 1A). As for the previously reported D-FF-OCT set-up, 10x water immersion microscope objectives were placed in the interferometer arms (Linnik configuration) to reach a transverse resolution of approximately 1.5 µm. Solid cultures (Figure 1B) were sampled and deposited on the upper slide of the apparatus sample holder according to an adapted protocol based on the tape touch method described elsewhere for fungal slide mounts [17]. The resulting fungal slides were then acquired following full-field illumination and subsequent dynamic contrast imaging with a complementary metal oxide semiconductor camera (Figure 1C). The penetration depth was adjusted to be approximately 100 µm and series of D-FF-OCT images with 1.5 µm spacing were recorded in depth.

2.3 Image analysis

ImageJ 1.49k software was used for axial z-stacking of multiple images and three-dimensional reconstruction (3D viewer plugin). Both FF-OCT standard and dynamic contrast image analysis with length measurements of different fungal compartments for each selected species were accessible using a contrast-based ImageJ 1.49k protocol called the "Plot Profile" Function. Regarding the specific analysis of dynamic contrast images, the time series associated to each pixel behavior was analyzed by a fast Fourier transform program. Then the spectrum was divided in three parts respectively associated to the three colors of the composite RGB images so that the highest frequencies (fast movements) correspond to the red color and the lowest frequencies to the bluer colors.

3 Results

3.1 D-FF-OCT observations of *Nannizzia gypsea*

The different aspects of NG are displayed in Figure 2. The two-dimensional structural FF-OCT image of NG from Figure 2A returns multiple thin and septate hyphae, most of the time longer than 200 µm, with a diameter ranging from 2 to 4 µm. Except for septa, the intensity of the FF-OCT signal is relatively comparable on the whole hyphae. The dynamic D-OCT image from Figure 2B confirms a similar shape of the NG hyphae with a homogenous and rather low dynamic contrast, from blue to pale green, no matter which septum of the septate hyphae. Three dimensional FF-OCT image of both hyphae and multicelled macroconidia are shown in Figure 2C. Macroconidia appear as fusiform structures approximately 50 µm-long and 15 µm-large with distinguishable septa (Figure 2C, white arrow). When compared to the bluish dynamic aspect of NG hyphae from Figure 2B, dynamic D-OCT image from Figure 2D shows intense orange dynamic contrast within the macroconidia of NG and outlines its multicelled structure.

3.2 D-FF-OCT observations of *Aspergillus fumigatus*

Acquisitions of AF solid cultures with D-FF-OCT are shown in Figure 3. As demonstrated by the two-dimensional image from Figure 3A, AF is composed of several septate conidiophores with length ranging from 200 to 300 µm and a diameter of 4-6 µm, slightly larger than the one from NG. When compared to the different compartments of NG, Figure 3A confirms a different FF-OCT signal between conidiophores, vesicles, phialides and conidia. The latter, with the smallest diameter of 2-4 µm, clearly show the brightest FF-OCT signal in comparison to the other parts of AF, notably vesicles. The two-dimensional dynamic D-OCT image displayed in Figure 3B highly contrasts with the corresponding structure image acquired with FF-OCT. Although the different sub-compartments display a morphology

comparable to the one from Figure 3A, both dynamic contrast and intensity enlighten complementary signature of each structure. First, the dynamic contrast can vary from pale blue to green or even yellow from one side of a conidiophore to another. In addition, vesicles most often display bright green-orange dynamic contrast, as compared to the pale bluish colors of the conidial heads or phialides. Finally, we see from Figure 3C that three-dimensional dynamic D-OCT image confirms the whole structure and dynamic contrast of both the conidiophores and conidial heads, approximately 50 µm-large.

3.3 D-FF-OCT observations of *Rhizopus arrhizus*

Results from D-FF-OCT observations of RA are presented in Figure 4. The three-dimensional FF-OCT view of RA sporangiophores from Figure 4A confirms a length above 300 µm for the longest and a diameter between 10 and 12 µm, without any septum. As for NG, the dynamic D-OCT image from Figure 4B confirms a similar shape of the RA sporangiophores with a homogenous and rather low dynamic contrast, from blue to pale green. Figure 4C precisely shows the dotted spherical shape and organization of RA sporangium, with a total diameter exceeding 100 µm. As for AF, the two-dimensional dynamic D-OCT image showing RA sporangiospores seems to highlight two compartments within the sporangium, each with a different contrast (Figure 4D): one in the center corresponding to the columellae, brighter and with enhanced contrast when compared to a second more peripherical area unfolding all sporangiospores.

4 Discussion

Except for a few reports describing the attempt to use standard OCT for the diagnosis of onychomycosis [11], dermatophytoma [18] as well as other applications in ophthalmology intended for the imaging of fungal keratitis [19] and chorioretinitis [20], there is to our knowledge no report of high definition D-FF-OCT imaging in fungal diagnostics. Indeed, the present study introduces the first observations of filamentous fungal species with D-FF-OCT, demonstrating the complementary potential of both high-definition structure (Figures 2A, C, Figure 3A and Figures 4A, C) and dynamic contrast (Figures 2B, D, Figures 3B, C and Figures 4B, D) images for the identification of fungi.

First, FF-OCT acquisitions return comparable information regarding the global structure of all three selected fungal species. In particular, the main characteristics of AF and RA with conventional microscopy largely correspond to the one obtained with FF-OCT: the thin branched and septate hyphae of AF (Figure 3A) are distinguishable from the larger pauci-septate RA sporangiophores displaying a ribbon-like structure (Figure 4A). A similar conclusion can be drawn from the comparison of AF conidial heads (Figure 3A) and the dotted spherical organization of RA sporangiospores (Figure 4C) hiding two compartments within the sporangium [6]. The observation of FF-OCT images of NG also confirms the typical ellipsoidal and thin-walled structure of NG multicelled macroconidia (Figure 2C), as for the usually reported microscopic examination and identification criteria [21]. Obviously, these results need to be confirmed on other fungal species to test the global performances and limits of such FF-OCT system for the identification of more precise morphological criteria usually dedicated to microbiological diagnostics: notably information such as the number of septa composing macroconidia or hyphae pigmentation.

In addition to such structural information, D-FF-OCT gave access to dynamic contrast imaging of fungal cells. Briefly, this technology was previously shown to provide complementary subcellular contrast to structural images obtained with FF-OCT. On the

suspected basis of mitochondria or cellular organelles movements, dynamic contrast has already demonstrated its ability to reflect both cell activity and metabolism [8]. Interestingly, the present data illustrate for the first time the exploitation of D-OCT to probe fungal subcellular dynamics. As shown in Figures 2B and D, the comparison of hyphae and macroconidia dynamic contrasts for NG very certainly reflects a different metabolic state of both structures [22]. In the case of NG, the intense orange dynamic contrast within the macroconidia may be the reflection of macroconidia metabolic activity (Figure 2D). Dynamic D-OCT images of AF show the same kind of opposition between vesicles or certain conidiophore segments displaying bright green-orange contrast and conidial heads or phialides associated with a paler bluish signal (Figures 3B, C). As for MF, these dynamic discrepancies in AF compartments very certainly correspond to a changing metabolic activity and signature of each fungal structure, also possibly occurring in the center of RA sporangium (Figure 4D). Still, additional experiments will be needed to better understand the exact nature of such dynamic contrast. Indeed, live-cell imaging of filamentous fungi mainly relies on the use of either cell wall or membrane selective dyes coupled with confocal laser scanning microscopy to analyze subcellular compartments dynamics and provide a better understanding of fungal morphogenesis [23,24]. A comparison of the signal obtained with D-OCT and live-cell imaging would help to better understand the origin of D-OCT dynamic contrast in fungi. Finally, given well known morphological discrepancies between *in vitro* and *in vivo* structural or even metabolic characteristics of fungi, the present D-FF-OCT-based visualization of non-dermatophytes filamentous species *in vitro* only constitutes the first attempt towards future works to better appreciate the morphological aspect of the same molds *in vivo*, throughout their parasitic phase, with deep-tissue D-FF-OCT imaging of direct clinical samples such as cutaneous, mucosal or lung biopsy.

5 Conclusion

Overall, this study introduces a novel application of D-FF-OCT for fungal diagnostics. Based on unprecedented structure and dynamic contrast imaging of three different fungal species, we bring conclusive evidence that such technology not only allows rapid identification of fungal compartments with a definition approaching conventional microscopy but also returns potential precious metabolic information regarding fungal subcellular dynamics, without any sample preparation, coloration, or any selective dye. Regarding clinical perspectives, it could serve rapid bedside extemporaneous analysis following nail scraping, skin biopsy as well as direct noninvasive *in vivo* histopathological examination of any skin or mucosal lesion within a few minutes, potentially helpful when compared to the actual time constraints associated with conventional preparations of histological sections (fixation, embedding, sectioning, staining) that sometimes require days of technical procedures and lead to significant delay in final diagnosis. Thus, we believe D-FF-OCT may serve as complementary tool for rapid IFI diagnosis in future microbiological laboratory and clinical routine practice. Further studies are needed to assess D-FF-OCT accuracy if applied to clinically relevant samples such as fresh tissues.

Figure captions

Fig. 1. D-FF-OCT set up for the acquisition of fungal solid cultures. (A) Global view of both hardware and software set up for fungal observations. (B) Fungal solid cultures exploited for D-FF-OCT observations. (C) Frontal view of the D-FF-OCT acquisition system with sample holder in the center. White arrow points the halogen source.

Fig. 2. D-FF-OCT observations of *Nannizzia gypsea*. (A) Two dimensional FF-OCT image showing *Nannizzia gypsea* hyphae. (B) Two dimensional D-OCT image showing *Nannizzia gypsea* hyphae. (C) Three dimensional FF-OCT image showing *Nannizzia gypsea* hyphae and macroconidia. (D) Three dimensional D-OCT image showing *Nannizzia gypsea* hyphae and macroconidia. Scale bar represents 50 µm. White arrow points the multicelled macroconidia.

Fig. 3. D-FF-OCT observations of *Aspergillus fumigatus*. (A) Two dimensional FF-OCT image showing *Aspergillus fumigatus* conidiophore and conidial heads. (B) Two dimensional D-OCT image showing *Aspergillus fumigatus* conidiophore and conidial heads. (C) Three dimensional D-OCT image showing *Aspergillus fumigatus* conidiophore and conidial heads. Scale bar represents 50 µm. White arrow points a conidial head of *Aspergillus fumigatus*.

Fig. 4. D-FF-OCT observations of *Rhizopus arrhizus*. (A) Three dimensional FF-OCT image showing *Rhizopus arrhizus* sporangiophores. (B) Three dimensional D-OCT image showing *Rhizopus arrhizus* sporangiophores. (C) Two dimensional FF-OCT image showing *Rhizopus arrhizus* sporangium and sporangiospores. (D) Two dimensional D-OCT image showing *Rhizopus arrhizus* sporangium and sporangiospores. Scale bar represents 50 µm.

Conflict of Interest

The authors declare that the research was conducted in the absence of any commercial or financial relationships that could be construed as a potential conflict of interest.

Author Contributions

TM and MS designed the study, conducted experiments, performed experimental works and wrote the manuscript. JMC, CB, DGH, FL and MS performed experimental works. JMC, CB, MB, LP, DGH, FL, MS and PEC contributed to the manuscript revision. TM, MS and FD supervised the project.

All authors contributed to the article and approved the submitted version.

Funding

This work was supported by crowdfunding (https://thellie.org/mycoct), by the WIFI labex and the HELMHOLTZ SYNERGY ERC PROGRAM.

Acknowledgments

We sincerely thank Beclere Corentin, Choux Isabelle, De Tardy De Montrave Françoise, Gitton Véronique, Laurenceau Raphaelle, Vincent Anne and Bailly Eloïse for their help regarding solid cultures of fungal species.

Data Availability Statement

All data from the study are included in the article. Further inquiries can be directed to the corresponding author.

References

[1] Chowdhary A, Sharma C, Meis JF. Azole-Resistant Aspergillosis: Epidemiology, Molecular Mechanisms, and Treatment. The Journal of Infectious Diseases 2017;216:S436–44. https://doi.org/10.1093/infdis/jix210.

[2] Danion F, Duréault A, Gautier C, Senechal A, Persat F, Bougnoux M-E, et al. Emergence of azole resistant-Aspergillus fumigatus infections during STAT3-deficiency. Journal of Medical Microbiology 2020;69:844–9. https://doi.org/10.1099/jmm.0.001200.

[3] Donnelly JP, Chen SC, Kauffman CA, Steinbach WJ, Baddley JW, Verweij PE, et al. Revision and Update of the Consensus Definitions of Invasive Fungal Disease From the European Organization for Research and Treatment of Cancer and the Mycoses Study Group Education and Research Consortium. Clinical Infectious Diseases 2020;71:1367–76. https://doi.org/10.1093/cid/ciz1008.

[4] Pruskowski KA, Mitchell TA, Kiley JL, Wellington T, Britton GW, Cancio LC. Diagnosis and Management of Invasive Fungal Wound Infections in Burn Patients. EBJ 2021;2:168–83. https://doi.org/10.3390/ebj2040013.

[5] Dekio F, Bhatti TR, Zhang SX, Sullivan KV. Positive Impact of Fungal Histopathology on Immunocompromised Pediatric Patients With Histology-Proven Invasive Fungal Infection. Am J Clin Pathol 2015;144:61–7. https://doi.org/10.1309/AJCPEMVYT88AVFKG.

[6] Antinori S, Corbellino M, Parravicini C. Challenges in the Diagnosis of Invasive Fungal Infections in Immunocompromised Hosts. Curr Fungal Infect Rep 2018;12:12–22. https://doi.org/10.1007/s12281-018-0306-0.

[7] Quénéhervé L, Olivier R, Gora MJ, Bossard C, Mosnier J-F, Benoit a la Guillaume E, et al. Full-field optical coherence tomography: novel imaging technique for extemporaneous high-resolution analysis of mucosal architecture in human gut biopsies. Gut 2021;70:6–8. https://doi.org/10.1136/gutjnl-2020-321228.

[8] Apelian C, Harms F, Thouvenin O, Boccara AC. Dynamic full field optical coherence tomography: subcellular metabolic contrast revealed in tissues by interferometric signals temporal analysis. Biomed Opt Express 2016;7:1511. https://doi.org/10.1364/BOE.7.001511.

[9] Dalimier E, Salomon D. Full-Field Optical Coherence Tomography: A New Technology for 3D High-Resolution Skin Imaging. Dermatology 2012;224:84–92. https://doi.org/10.1159/000337423.

[10] Maldiney T, Greigert H, Martin L, Benoit E, Creuzot-Garcher C, Gabrielle P-H, et al. Full-field optical coherence tomography for the diagnosis of giant cell arteritis. PLoS ONE 2020;15:e0234165. https://doi.org/10.1371/journal.pone.0234165.

[11] Olsen J, Lindsø Andersen P, Themstrup L, Jemec GBE, Saunte DML. Optical coherence tomography of onychomycosis: proposed terminology and a suggestion of practical usage. Arch Dermatol Res 2020;312:51–8. https://doi.org/10.1007/s00403-019-01989-8.

[12] van Manen L, Dijkstra J, Boccara C, Benoit E, Vahrmeijer AL, Gora MJ, et al. The clinical usefulness of optical coherence tomography during cancer interventions. J Cancer Res Clin Oncol 2018;144:1967–90. https://doi.org/10.1007/s00432-018-2690-9.

[13] Andersen AJB, Fuchs C, Ardigo M, Haedersdal M, Mogensen M. In vivo characterization of pustules in Malassezia Folliculitis by reflectance confocal

microscopy and optical coherence tomography. A case series study. Skin Res Technol 2018;24:535–41. https://doi.org/10.1111/srt.12463.

[14] Morsy H, Mogensen M, Thomsen J, Thrane L, Andersen PE, Jemec GBE. Imaging of cutaneous larva migrans by optical coherence tomography. Travel Medicine and Infectious Disease 2007;5:243–6. https://doi.org/10.1016/j.tmaid.2006.12.004.

[15] Banzhaf CA, Themstrup L, Ring HC, Welzel J, Mogensen M, Jemec GBE. In vivo Imaging of ***Sarcoptes scabiei*** Infestation Using Optical Coherence Tomography. Case Rep Dermatol 2013;5:156–62. https://doi.org/10.1159/000352066.

[16] Ghouali W, Grieve K, Bellefqih S, Sandali O, Harms F, Laroche L, et al. Full-Field Optical Coherence Tomography of Human Donor and Pathological Corneas. Current Eye Research 2015;40:526–34. https://doi.org/10.3109/02713683.2014.935444.

[17] Harris JL. Safe, low-distortion tape touch method for fungal slide mounts. J Clin Microbiol 2000;38:4683–4. https://doi.org/10.1128/JCM.38.12.4683-4684.2000.

[18] Verne SH, Chen L, Shah V, Nouri K, Tosti A. Optical Coherence Tomography Features of Dermatophytoma. JAMA Dermatol 2018;154:225. https://doi.org/10.1001/jamadermatol.2017.4590.

[19] Sharma N, Singhal D, Maharana PK, Agarwal T, Sinha R, Satpathy G, et al. Spectral Domain Anterior Segment Optical Coherence Tomography in Fungal Keratitis. Cornea 2018;37:1388–94. https://doi.org/10.1097/ICO.0000000000001715.

[20] Adam MK, Rahimy E. Enhanced Depth Imaging Optical Coherence Tomography of Endogenous Fungal Chorioretinitis. JAMA Ophthalmol 2015;133:e151931. https://doi.org/10.1001/jamaophthalmol.2015.1931.

[21] Mohamed Shalaby MF, Nasr El-din A, Abu El-Hamd M. Isolation, Identification, and In Vitro Antifungal Susceptibility Testing of Dermatophytes from Clinical Samples at Sohag University Hospital in Egypt. Electron Physician 2016;8:2557–67. https://doi.org/10.19082/2557.

[22] Dill BC, Leighton TJ, Stock JJ. Physiological and biochemical changes associated with macroconidial germination in Microsporum gypseum. Appl Microbiol 1972;24:977–85. https://doi.org/10.1128/am.24.6.977-985.1972.

[23] Lichius A, Zeilinger S. Application of Membrane and Cell Wall Selective Fluorescent Dyes for Live-Cell Imaging of Filamentous Fungi. JoVE 2019:60613. https://doi.org/10.3791/60613.

[24] Pfister J, Lichius A, Summer D, Haas H, Kanagasundaram T, Kopka K, et al. Live-cell imaging with Aspergillus fumigatus-specific fluorescent siderophore conjugates. Sci Rep 2020;10:15519. https://doi.org/10.1038/s41598-020-72452-2.

(A)

(B)

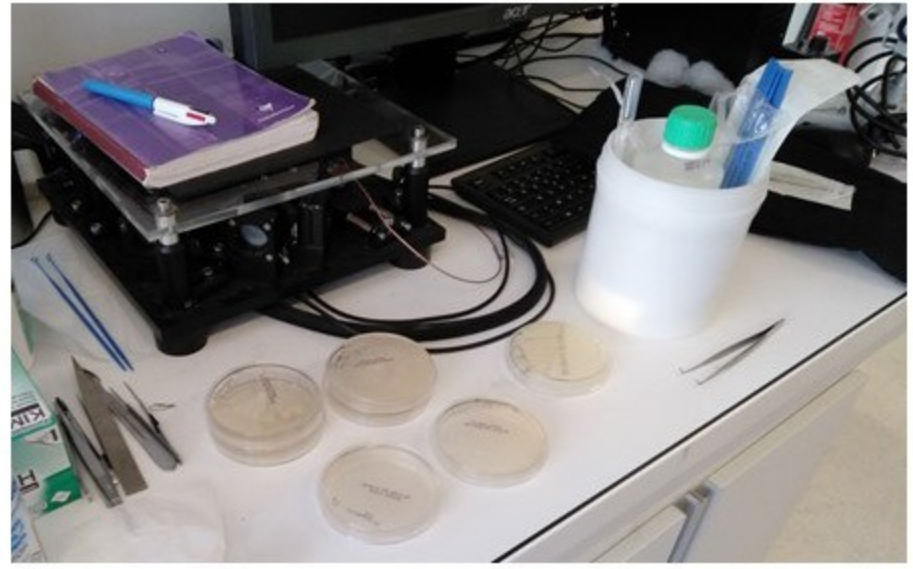

(C)

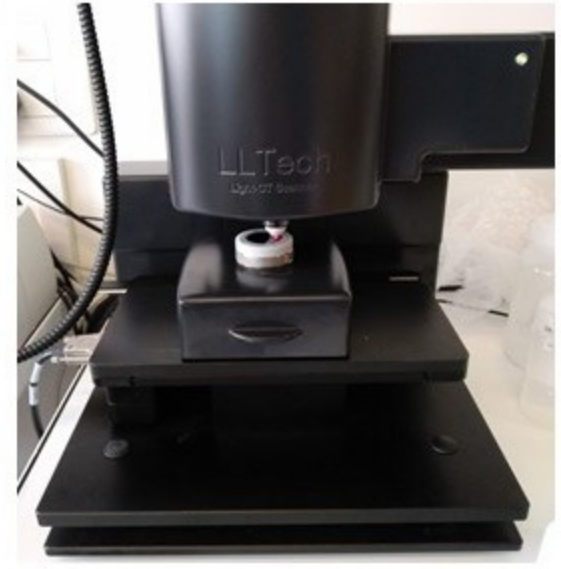

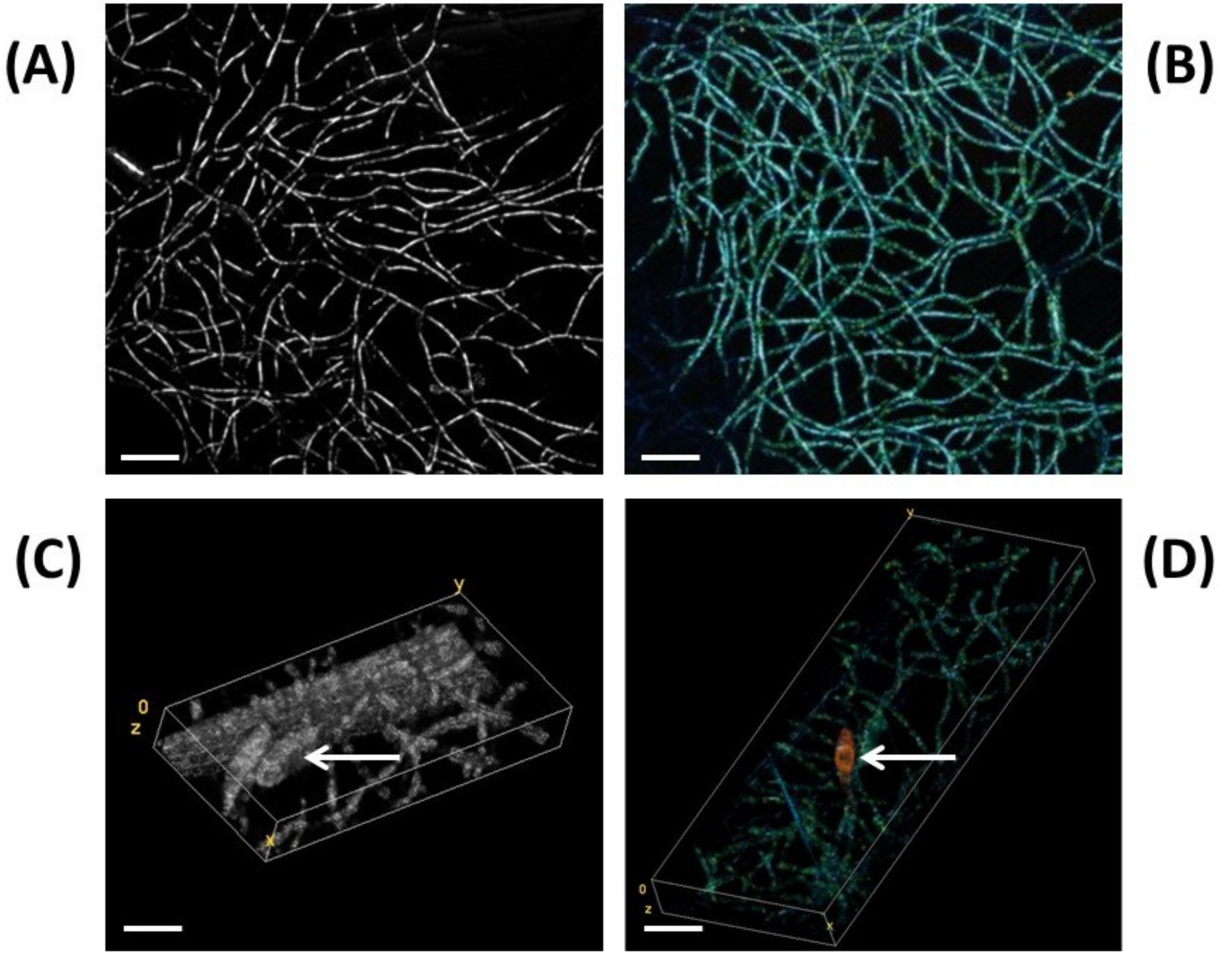
(A)
(B)
(C)
(D)
y
0
z
x
y
0
z
x

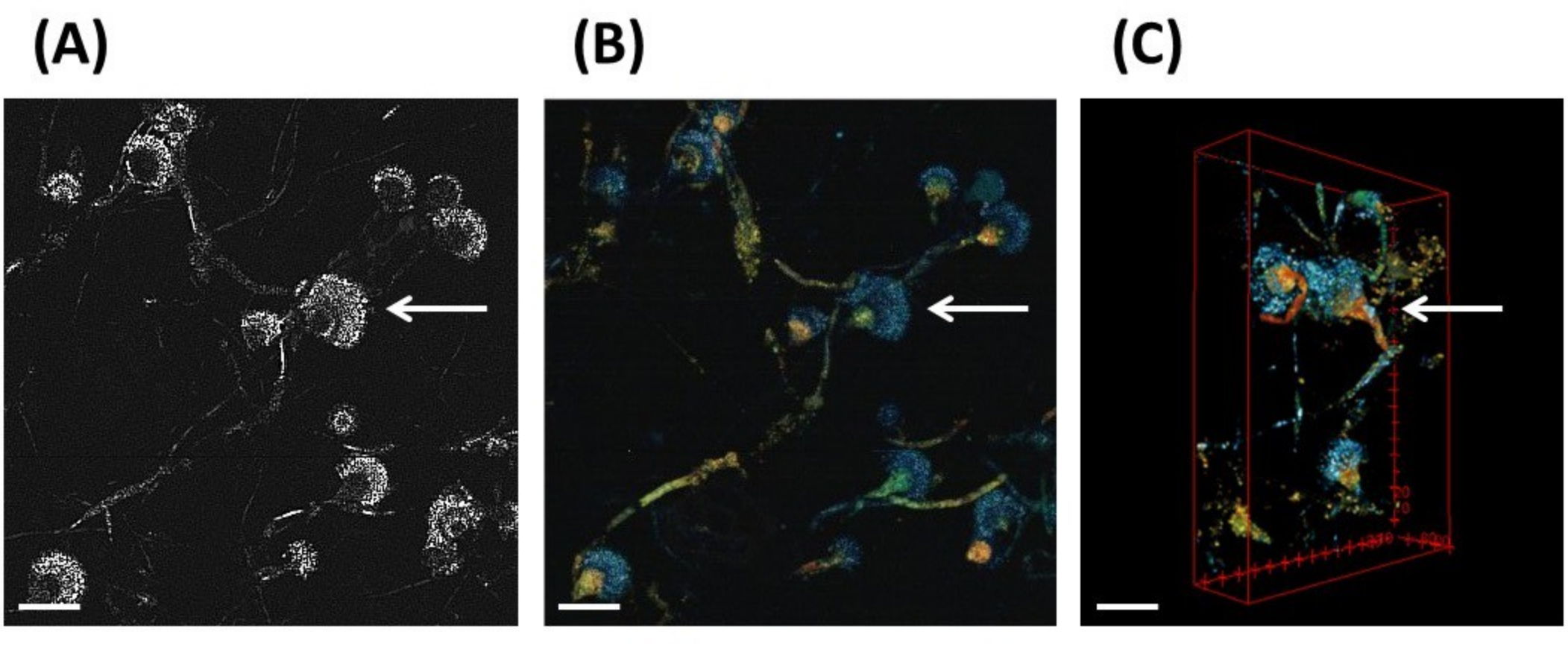
(A)
(B)
(C)

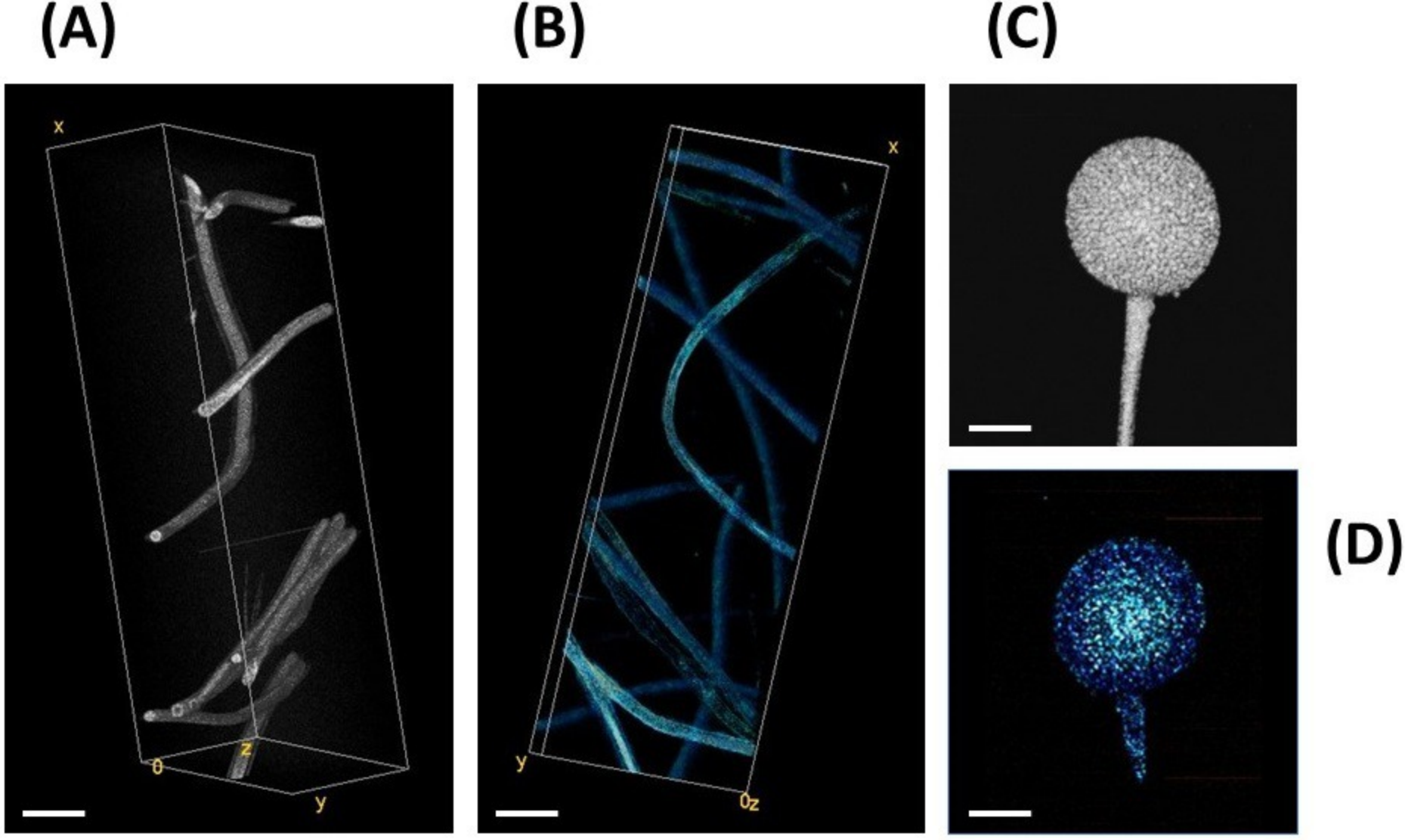
(A)
(B)
(C)
(D)
x
z
0
y
x
y
0z